PCCP

Accepted Manuscript

This is an *Accepted Manuscript*, which has been through the Royal Society of Chemistry peer review process and has been accepted for publication.

Accepted Manuscripts are published online shortly after acceptance, before technical editing, formatting and proof reading. Using this free service, authors can make their results available to the community, in citable form, before we publish the edited article. We will replace this *Accepted Manuscript* with the edited and formatted *Advance Article* as soon as it is available.

You can find more information about *Accepted Manuscripts* in the **Information for Authors**.

Journal Name

Unique Raman fingerprint of Boron Nitride Substitution Patterns in Graphene†

Lorenzo Maschio,[*a,c] Marco Lorenz,[a‡] Daniele Pullini,[b] Mauro Sgroi,[b] and Bartolomeo Civalleri,[a,c]

Boron Nitride-substituted Graphene (BNsG) two-dimensional structures are new materials of wide technological interest due to the rich variety of electronic structures and properties they can exploit. The ability to accurately characterize them is key to their future success.

Here we show, by means of *ab initio* simulations, that the vibrational Raman spectra of such compounds are extremely sensitive to substitution motifs and concentration, and that each structure has unique and distinct features. This result can be useful as a guide for the optimization of production processes.

1 Introduction

Much of current research in the field of materials science is focused on nanostructures derived from graphene.[1–9] In this wide field, one topic that attracted considerable interest is the study of a possible relationship between hexagonal Boron nitride (h-BN) and graphene, either as separate or combined sheets. In fact, h-BN can be adopted as a substrate to support graphene, considered they have the same honeycomb lattice and a small mismatch in lattice parameters.[10] Extremely interesting novel physical properties arise then from the formation of Moiré superlattices.[11–13] On the other hand, BN-molecules can be included in the graphene structure by replacing C_2-pairs, allowing for opening up a band gap up to a fraction of the one of hexagonal BN (h-BN) itself (5.97 eV[14]).

Another field of rising interest is the construction of one-dimensional structures from graphene, the so-called graphene nanoribbons (GNRs):[15–18] these exploit very interesting electronic properties that can be tuned by controlling size and shape of the stripes.[5,19–23] They can be constructed with good control by unzipping or cutting open Carbon Nanotubes (CNTs),[15,16] by graphite nanotomy,[24] on-surface synthesis[25] or even grown inside nanotubes.[26]

The present work focuses on the *ab initio* modelling of 2D structures combining graphene and boron nitride in tailored specific geometries (hereinafter: BN substituted graphene, BNsG) with properties comparable to graphene nanoribbons and possibly easier to be fabricated. The topic has been previously investigated: several computational works have focused on it[27–35] as well as few experimental studies,[36–38] all growing graphene heterostructures via chemical vapor deposition (CVD). From a theoretical point of view,[39] it has been demonstrated that graphene/h-BN interfaces can lead to polar discontinuities, resulting in the formation of macroscopic dipoles. Such dipoles can definitely have an effect on the vibrational properties of the materials. Experimentally, an island–like motif is found to be thermodynamically the most stable structure.[36,37,40] It appears however difficult to avoid unexpected doping effects in the respective islands,[36] and at the same time the confinement of devices to the nanoscale is limited by the island size. A more recent CVD-approach[37] suggests that different small-sized BN-islands can be created in the graphene structure. Recent findings[41] also indicate that one dimensional h-BN/Graphene can be built from heteroepitaxial growth. A different approach has been recently proposed: it implies the creation of vacancies of C atoms in the regular structure of graphene layers.[42] Those defects could be saturated with heteroatoms like boron and nitrogen, representing a viable solution to fabricate

a Dipartimento di Chimica, Università di Torino, via Giuria 5, I-10125 Torino (Italy); E-mail: lorenzo.maschio@unito.it

b Centro Ricerche FIAT, Strada Torino 50, 10043 Orbassano, Torino (Italy)

c NIS (Nanostructured Interfaces and Surfaces) Centre, Università di Torino, via Giuria 5, I-10125 Torino (Italy)

† Electronic Supplementary Information (ESI) available: [details of any supplementary information available should be included here]. See DOI: 10.1039/b000000x/

BNsG with full control on different patterns, by using CVD heteroepitaxy.

Raman spectroscopy has historically played an important role in the structural characterization of graphitic materials,[43–45] and their disorder.[46] Raman spectroscopy is – in fact – a relatively cheap, commonly available, nondestructive technique which is widely used for investigating Graphene properties.[12,47] The application of such technique in the study of BNsG structures has seen considerably less success,[36] we believe due to the lack of reference spectra other than pure graphene or h-BN, to serve as a guide in the interpretation.

Here we intend to fill this gap by reporting a systematic study of simulated Raman spectra of different substitution patterns in BNsG. As we have found in the present work, Raman spectroscopy potentially represents an extremely powerful tool for the characterization of such materials (*vide infra*). Moreover, at difference with respect to previous studies focused on electronic structures of BNsG structures,[27] we have used of a hybrid functional augmented with an empirical dispersion correction.[48,49] The adopted quantum chemical treatment allows for a better prediction of both structures and band gaps. For band gaps, this leads to computed values that are at least two times larger than in previous studies in which semilocal functionals were employed.[27]

2   Theoretical methods and models

The structures considered in this work are reported in Fig. 1. For a given pattern, the amount of BN substitutions is allowed to vary the BN-part from maximally 75% down to minimally 6%. For our calculations we utilized the CRYSTAL14 *ab initio* code[50] adopting a hybrid HF/DFT functional (i.e. B3LYP). Hybrid functionals are known to outperform more commonly used semilocal functionals in the prediction of band gaps and structures (see supplementary data[51]) as well as vibrational properties. In Table 1 we report the position of the E_{2g} band of the Raman spectrum of the pristine h-BN and graphene monolayer systems. It is seen that among all tested functionals (that include local, gradient-generalized, dispersion-corrected, global and range-separated hybrids) B3LYP, along with PBE, shows the best performance. A correction for missing dispersion interactions is also included.[52–57] The code allows for fully analytical evaluation of Raman intensities,[58] thus constituting a convenient tool for the simulation of vibrational spectra. The approach is based on a double-harmonic approximation for the vibrational frequencies (peak positions) and a coupled-perturbed approach is used to evaluate the intensities.[58]

An all-electron 6-31g(d,p) basis set has been used on all atoms. Very tight values (7 7 7 15 80) have been chosen for the five CRYSTAL14 integral screening tolerances (see Ref.[50] and reference therein) to ensure best accuracy. Very dense k-space meshes (up to 48×48 k-points for the smallest unit cells) have been selected for the same purpose.

	Graphene	h-BN layer
LDA	1620	1395
PBE	1574	1348
B3LYP	1609	1374
B3LYP-D	1608	1376
HSE0	1641	1399
Exp.	1582[59]	1369[60,61]

Table 1: Computed Raman-active E_{2g} vibrational frequencies (in cm^{-1}) of pristine graphene and h-BN (both in the 3D bulk and 2D single layer case), with comparison to the experimental values.

3   Results and discussion

In Figure 2 we report the simulated Raman spectra for the different structures considered, subdivided in three panels according to the pattern type. The "island" patterns are most easily found experimentally, as reported by Ci *et al.*,[36] and an experimental Raman spectrum is also available, that we also report in the top panel of Fig. 2. Notably, the whole set of simulated spectra matches well the main features of the experimental profile. The 48% and 19% substitutions, in particular, reproduce the broad peak around 1300 cm^{-1} (corresponding to the zone of the D band) and also the small peaks above 1600 cm^{-1} correctly reproduce the shoulder (D' band) on the right slope of the broad G band.

In the middle panel of Figure 2 we report the simulated spectra relative to the most interesting nanostructures – the zigzag ones, forming in-plane Carbon nanoribbons. We see that the spectra are definitely different from all other structures: The region around 1500 cm^{-1}, that shows very low intensities in the Island–type defects (and nearly no significant peaks in the Armchair defects – see below), features here significant peaks in all concentrations, with positions depending on the concentration itself. For lower BN concentrations he fragmentation of the graphene G band around 1580 cm^{-1} is less pronounced than in other structures. Nearly no features are present below 1400 cm^{-1}.

In the bottom panel of Figure 2 we can see that the overall appearance of Raman features for Armchair structures resembles that of "Island" ones, with relatively more intense peaks in the D–band region. The total absence of intense peaks in the 1400–1500 cm^{-1} region is a characteristic that marks this type of defect, as well as as the shifting of the above mentioned D–band features towards lower wavenumbers.

Let us now focus on the electronic properties of different substitutions patterns. Since graphene is usually grown on a substrate, we also took a step forward to reality and included h-BN as a support. In Figure 3 (a) we report the computed band gaps for different amount of substitutions and patterns of BN in graphene

Fig. 1: Details of the considered structural models of BNsG using their minimal supercells. Carbon is black, boron blue, and nitrogen salmon. Zigzag2 (2b) and Armchair2 (3b) are equivalent using minimal supercells, i.e. 25% BN substitutions, but are different for lower amounts of substitutions/larger supercells. The red circles in (1b) and (1c) emphasize the size of the Islands (two and three concentric circles of BN).
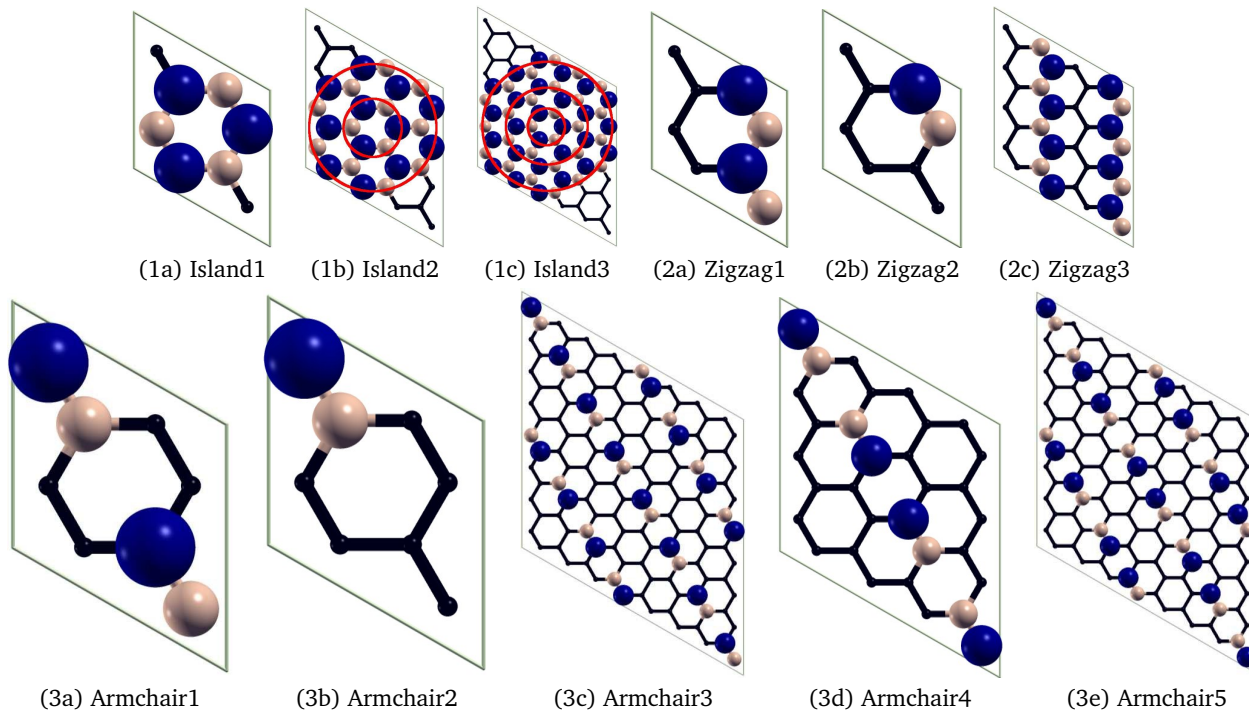

(1a) Island1   (1b) Island2   (1c) Island3   (2a) Zigzag1   (2b) Zigzag2   (2c) Zigzag3

(3a) Armchair1   (3b) Armchair2   (3c) Armchair3   (3d) Armchair4   (3e) Armchair5

Fig. 3: Band gaps of BNsG and BNsG supported by h-BN. The maximum of the ordinate is set to the band gap of h-BN (5.97 eV [14]) Points on the dashed black line correspond to a linear increase of the band gap with the amount of BN-substitutions, e.g. 50% substitutions correspond to 50% of the band gap of h-BN.
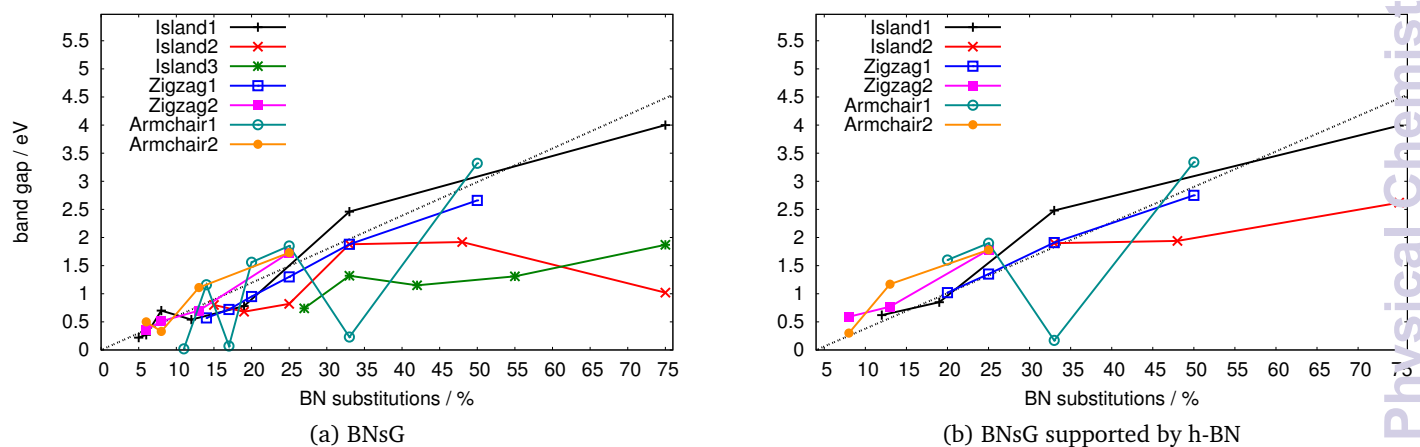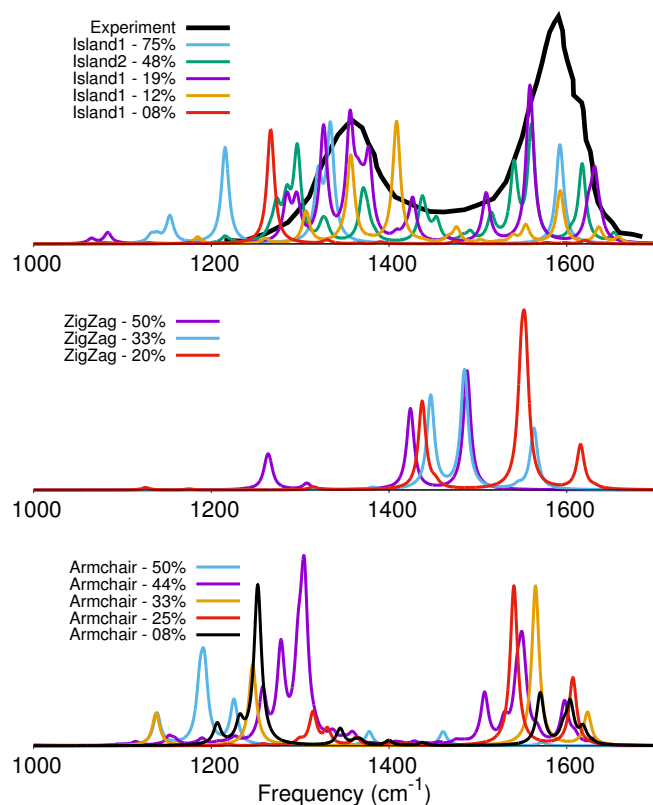

(a) BNsG   (b) BNsG supported by h-BN

Fig. 2: Simulated Raman spectra of BNsG structures at different BN-substitutions. In the top panel, the experimental spectrum from Ci *et al.*[36] has been reported. Intensity in arbitrary units.

for both the supported and stand-alone sheets (see Fig. 1 for labelling). Over the whole range of substitutions we investigated, different patterns show a wide heterogeneity of band gaps, but none of them is significantly influenced by the support on h-BN.

We found that the convexity of Island patterns in the area between about 10% and 30% leads to a smaller band gap compared to linear patterns. This makes in-line patterns especially interesting when aiming for a moderate number of BN-substitutions. Variations of about 1 eV (medium amount of substitutions) up to several eV (high amount) are observed. In most cases, increasing the amount of BN portion does lead to quasi-linear increase of the band gap. There some peculiarities appear, for instance, the Island3 shows at 75% a smaller band gap than at 33%, which might be attributed to the spacing between the BN-islands[34]. The largest band gap is opened by the Island1 pattern at 75%, reaching 67% of the band gap of h-BN. At 25% substitutions, the Armchair1 pattern shows the highest band gap (1.85 eV), while Island2 accounts for the minimal band gap (0.83 eV). At 50% sub-

stitutions, where the material can barely be called BNsG, for the Armchair1 pattern a gap up to 3.32 eV can be opened, that falls in the UV part of light spectrum.

Interestingly, the Armchair and Zigzag patterns can be seen as an infinite number of armchair and zigzag GNRs strung together, respectively. In armchair GNRs (acGNRs) the band gap is very small when the width of the GNR is $3(p-1)+2$ (p is a positive integer)[5,62]. The Armchair1 pattern shows the same behaviour: the band gap at 11% (width 8), 17% (width 5) and 33% (width 2) is virtually zero, while at slightly different BN amount of, for instance, 14% (width 6) the band gap is 1.16 eV. Such non monotonic behavior was not observed in a previous studiy by other authors.[27] The Zigzag patterns in Fig. 1 – as corresponding to the zigzag GNRs – show only a dependency on the amount of BN-substitutions, leading to a nearly linear increase of the band gap. Armchair2 can be seen as a variation of the Zigzag pattern with a certain spacing between the BN-entities, e.g. at 25% it is equivalent to Zigzag2, and therefore shows also a linear increase of the band gap. At 50% substitutions, the band gap of Zigzag1 seems a bit damped, which might indicate a saturation.

The relative formation energies for BN-substitutions, $E_{\mathrm{rFE}}(\text{BN-subs})$, are creported in Figure 4. These were computed via the following formula:

$$E_{\mathrm{rFE}}(\text{BN-subs}) = E(\text{BN-subs}) - \left(N_{\text{C-atoms}} \times E_{\text{C-atom}} \right.$$

$$\left. + N_{\text{B/N-atoms}} \times \left(E_{\text{B-atom}} + E_{\text{N-atom}} \right) \right) - E_{\text{inter}} \quad ,$$

$$(1)$$

where $E(\text{BN-subs})$ is the electronic energy of BN-substituted graphene at a given pattern and concentration of defects, $N_{\text{C-atoms}}$ and $N_{\text{B/N-atoms}}$ are the number of carbon and boron/nitrogen atoms in this structure, respectively, and $E_{\text{C-atom}}$ (same for B and N) is the electronic energy of a single carbon (boron, nitrogen) atom. E_{inter} is the energy gained from a linear interpolation between pure graphene and pure h-BN. We do not consider vibrational and entropic contributions.

Fig. 4: Relative formation energies for different patterns and amounts of BN-substitutions.
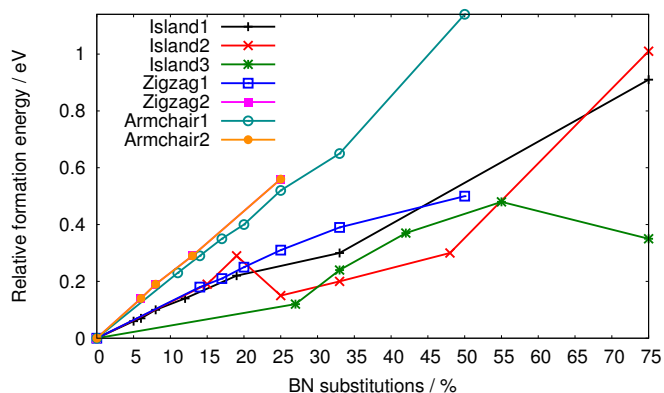
In agreement with literature [36,37,40] we find that the electronic part of the relative formation energies show that in-line patterns are disfavoured with respect to circular patterns.

In the Supplementary Information [51] we report further characterization of these structures, like band structures and Density of States (DOS).

4 Summary and conclusions

In conclusion, our work lays the foundation to understanding the distinctive features in the Raman spectrum of different type of BN substitution motifs (island, zigzag, armchair) in graphene. In particular, it is striking to see that the appearance of peaks in the region between 1400 and 1500 cm-1 is a clear indication of the presence of "zigzag" patterns. This emphasizes how such result can be useful to guide the characterization and synthesis of such materials. Beside, we show that small to intermediate in-line patterns open a wider band gap than circular patterns. Remarkably, armchair1 and Zigzag1 BNsG can really be seen as 2D-periodic heterostructure analogs of armchair and zigzag graphene nanoribbons, framed by BN-entities. The Armchair1 BNsG show a close-to-zero band gap at a width of 3(p - 1) + 2 (p positive integer), while a wide band gap is predicted otherwise. The effect of a h-BN substrate is shown to be negligible for the properties of interest here. According to our data about the relative stabilities of different patterns, it should not be difficult to synthesize the in-line structures. The present work thus provides unique insights to precisely establish structure-property trends in BN substituted graphene.

5 acknowledgments

References

1 K. S. Novoselov, A. K. Geim, S. V. Morozov, D. Jiang, Y. Zhang, S. V. Dubonos, I. V. Grigorieva and A. A. Firsov, *Science*, 2004, **306**, 666–669.

2 J. C. Meyer, A. K. Geim, M. I. Katsnelson, K. S. Novoselov, T. J. Booth and S. Roth, *Nature*, 2007, **446**, 60–63.

3 A. K. Geim and K. S. Novoselov, *Nature Materials*, 2007, **6**, 183 – 191.

4 V. Barone, O. Hod and G. E. Scuseria, *Nano Lett.*, 2006, **6**, 2748–2754.

5 S. Dutta and S. K. Pati, *J. Mater. Chem.*, 2010, **20**, 8207–8223.

6 A. Du, Z. Zhu and S. C. Smith, *J Am Chem Soc.*, 2010, **132**, 2876–2877.

7 J. Lahiri, Y. Lin, P. Bozkurt, I. I. Oleynik and M. Batzill, *Nature Nanotechnology*, 2010, **5**, 326–329.

8 W. Oswald and Z. Wu, *Phys. Rev. B*, 2012, **85**, 115431.

9 M. De La Pierre, P. Karamanis, J. Baima, R. Orlando, C. Pouchan and R. Dovesi, *J. Phys. Chem. C*, 2013, **117**, 2222–2229.

10 G. Giovannetti, P. A. Khomyakov, G. Brocks, P. J. Kelly and J. van den Brink, *Phys. Rev. B*, 2007, **76**, 073103.

11 M. Yankowitz, J. Xue, D. Cormode, J. D. Sanchez-Yamagishi, K. Watanabe, T. Taniguchi, P. Jarillo-Herrero, P. Jacquod and B. J. LeRoy, *Nature Physics*, 2012, **8**, 382–386.

12 A. Eckmann, J. Park, H. Yang, D. Elias, A. S. Mayorov, G. Yu, R. Jalil, K. S. Novoselov, R. V. Gorbachev, M. Lazzeri, A. K. Geim and C. Casiraghi, *Nano Lett.*, 2013, **13**, 5242–5246.

13 M. Neek-Amal and F. M. Peeters, *Appl. Phys. Lett*, 2014, **104**, year.

14 K. Watanabe, T. Taniguchi and H. Kanda, *Nature Materials*, 2004, **3**, 404 – 409.

15 D. V. Kosynkin, A. L. Higginbotham, A. Sinitskii, J. R. Lomeda, A. Dimiev, B. K. Price and J. M. Tour, *Nature*, 2009, **458**, 872–876.

16 L. Jiao, L. Zhang, X. Wang, G. Diankov and H. Dai, *Nature*, 2009, **458**, 877–880.

17 J. Cai, P. Ruffieux, R. Jaafar, M. Bieri, T. Braun, S. Blankenburg, M. Muoth, A. P. Seitsonen, M. Saleh, X. Feng, K. Mãijllen and R. Fasel, *Nature*, 2010, **466**, 470–473.

18 L. Jiao, X. Wang, G. Diankov, H. Wang and H. Dai, *Nature Nanotechnology*, 2010, **5**, 321 – 325.

19 S. Dutta, A. K. Manna and S. K. Pati, *Phys. Rev. Lett.*, 2009, **102**, 096601.

20 M. Wang and C. M. Li, *Nanoscale*, 2011, **3**, 2324–2328.

21 A. K. Manna and S. K. Pati, *J. Mater. Chem. C*, 2013, **1**, 3439–3447.

22 L. Ma, J. Wang and F. Ding, *ChemPhysChem*, 2013, **14**, 47–54.

23 P. Wu, Q. Wang, G. Cao, F. Tang and M. Huang, *Physics Letters A*, 2014, **378**, 817–821.

24 N. Mohanty, D. Moore, Z. Xu, T. Sreeprasad, A. Nagaraja, A. A. Rodriguez and V. Berry, *Nature Communications*, 2012, **3**, 844.

25 P. Ruffieux, J. Cai, N. C. Plumb, L. Patthey, D. Prezzi, A. Ferretti, E. Molinari, X. Feng, K. Müllen, C. A. Pignedoli and R. Fasel, *ACS Nano*, 2012, **6**, 6930–6935.

26 A. V. Talyzin, I. V. Anoshkin, A. V. Krasheninnikov, R. M. Nieminen, A. G. Nasibulin, H. Jiang and E. I. Kauppinen, *Nano Lett.*, 2011, **11**, 4352–4356.

27 P. P. Shinde and V. Kumar, *Phys. Rev. B*, 2011, **84**, 125401.

28 X. Fan, Z. Shen, A. Q. Liuc and J.-L. Kuo, *Nanoscale*, 2012, **4**, 2157–2165.

29 Q. Peng and S. De, *Physica E: Low-dimensional Systems and Nanostructures*, 2012, **44**, 1662–1666.

30 R. Zhao, J. Wang, M. Yang, Z. Liu and Z. Liu, *J. Phys. Chem. C*, 2012, **116**, 21098–21103.

31 S. Suzuki and H. Hibino, *Materials Science and Engineering: B*, 2012, **177**, 233–238.

32 Z. Huang, V. H. Crespi and J. R. Chelikowsky, *Phys. Rev. B*, 2013, **88**, 235425.

33 P. Rani and V. K. Jindal, *RSC Adv.*, 2013, **3**, 802–812.

34 J. Wang, R. Zhao, M. Yang, Z. Liu and Z. Liu, *J. Chem. Phys.*, 2013, **138**, 084701.

35 P. Nath, S. Chowdhury, D. Sanyal and D. Jana, *Carbon*, 2011, **73**, 275–282.

36 L. Ci, L. Song, C. Jin, D. Jariwala, D. Wu, Y. Li, A. Srivastava, Z. F. Wang, K. Storr, L. Balicas, F. Liu and P. M. Ajayan, *Nature Materials*, 2010, **9**, 430–435.

37 G. Bepete, D. Voiry, M. Chhowalla, Z. Chiguvare and N. J. Coville, *Nanoscale*, 2013, **5**, 6552–6557.

38 B. Muchharla, A. Pathak, Z. Liu, L. Song, T. Jayasekera, S. Kar, R. Vajtai, L. Balicas, P. M. Ajayan, S. Talapatra and N. Ali, *Nano Lett.*, 2013, **13**, 3476–3481.

39 M. Gibertini, G. Pizzi and N. Marzari, *Nature Communications*, 2014, **5**, 5157.

40 K. Yuge, *Phys. Rev. B*, 2009, **79**, 144109.

41 L. Liu, J. Park, D. A. Siegel, K. F. McCarty, K. W. Clark, W. Deng, L. Basile, J. C. Idrobo, A.-P. Li and G. Gu, *Science*, 2014, **343**, 163–167.

42 M. M. Ugeda, D. Fernández-Torre, I. Brihuega, P. Pou, A. J. Martínez-Galera, R. Pèrez and J. M. Gómez-Rodríguez, *Phys. Rev. Lett.*, 2011, **107**, 116803.

43 M. S. Dresselhaus, G. Dresselhaus, K. Sugihara, I. L. Spain and H. A. Goldberg, in *Graphite Fibers and Filaments*, ed. B. Springer-Verlag, 1988, vol. 5.

44 M. S. Dresselhaus, G. Dresselhaus, R. Saito and A. Jorio, *Phys. Rep.*, 2005, **409**, 47–99.

45 Z. H. Ni, T. Yu, Y. H. Lu, Y. Y. Wang, Y. P. Feng and Z. X. Shen, *ACS Nano*, 2008, **2**, 2301–2305.

46 M. A. Pimenta, G. Dresselhaus, M. S. Dresselhaus, L. G. Cancado, A. Jorio and R. Saito, *Phys. Chem. Chem. Phys.*, 2007, **9**, 1276–1290.

47 C. Casiraghi, *Raman spectroscopy of graphene*, RSC Publishing, 2012, vol. 43.

48 S. Grimme, *Journal of Computational Chemistry*, 2006, **27**, 1787–1799.

49 B. Civalleri, C. M. Zicovich-Wilson, L. Valenzano and P. Ugliengo, *CrystEngComm*, 2008, **10**, 405–410.

50 R. Dovesi, R. Orlando, A. Erba, C. M. Zicovich-Wilson, B. Civalleri, S. Casassa, L. Maschio, M. Ferrabone, M. De La Pierre, P. D'Arco, Y. Noẽ́l, M. Causã̌, M. Rérat and B. Kirtman, *International Journal of Quantum Chemistry*, 2014.

51 See Supplementary Material Document No._____ for specification of the structural parameters, basis sets and computational details.

52 Y. Noel, P. D'arco, R. Demichelis, C. M. Zicovich-Wilson and R. Dovesi, *Journal of Computational Chemistry*, 2010, **31**, 855–862.

53 R. Demichelis, B. Civalleri, M. Ferrabone and R. Dovesi, *International Journal of Quantum Chemistry*, 2010, **110**, 406–415.

54 R. Demichelis, Y. Noël, P. Ugliengo, C. M. Zicovich-Wilson and R. Dovesi, *J. Phys. Chem. C*, 2011, **115**, 13107–13134.

55 R. Orlando, R. Bast, K. Ruud, U. Ekström, M. Ferrabone, B. Kirtman and R. Dovesi, *J Phys Chem A*, 2011, **115**, 12631–12637.

56 M. Ferrabone, B. Kirtman, M. Rérat, R. Orlando and R. Dovesi, *Phys. Rev. B*, 2011, **83**, 235421.

57 M. Ferrabone, B. Kirtman, V. Lacivita, M. Rérat, R. Orlando and R. Dovesi, *International Journal of Quantum Chemistry*, 2012, **112**, 2160–2170.

58 L. Maschio, B. Kirtman, M. R'erat, R. Orlando and R. Dovesi, *J. Chem. Phys.*, 2013, **139**, 164102.

59 L. Malard, M. Pimenta, G. Dresselhaus and M. Dresselhaus, *Physics Reports*, 2009, **473**, 51 – 87.

60 R. Arenal, A. C. Ferrari, S. Reich, L. Wirtz, J.-Y. Mevellec, S. Lefrant, A. Rubio, and A. Loiseau, *Nano Letters*, 2006, **6**, 1812–1816.

61 R. V. Gorbachev, I. Riaz, R. R. Nair, R. Jalil, L. Britnell, B. D. Belle, E. W. Hill, K. S. Novoselov, K. Watanabe, T. Taniguchi, A. K. Geim and P. Blake, *Small*, 2011, **7**, 465–468.

62 H. Raza and E. C. Kan, *Phys. Rev. B*, 2008, **77**, 245434.

63 A. Kokalj, *Comp. Mater. Sci.*, 2003, **28**, 155–168.

64 T. Williams, C. Kelley and many others, *Gnuplot 4.6: an interactive plotting program*, 2012.